

X-ray luminosity versus orbital period of AM CVn systems

Teja Begari¹ and Thomas J. Maccarone²

¹Independent Scientist, Hyderabad, India, begariteja@gmail.com

²Department of Physics & Astronomy, Texas Tech University,
Lubbock TX 79409

Abstract

AM CVn systems are a rare type of cataclysmic variable star consisting of a white dwarf accreting material from a low-mass, hydrogen-poor donor star. These helium-rich systems usually have orbital periods that are less than 65 minutes and are predicted to be sources of gravitational waves. We have analyzed the catalogued X-ray data from the Chandra, XMM-Newton, and The Neil Gehrels Swift Observatory (hereafter referred to as 'Swift') to investigate the relationship between X-ray luminosity and the orbital period of AM CVn systems. We find that the high accretion-rate systems which are likely to have optically thick boundary layers are sub-luminous in X-rays relative to theoretical model predictions for the boundary layer luminosity, while the longer orbital period, lower bolometric luminosity systems match fairly well to the model predictions, with the exception of an overluminous system which has already been suggested to show magnetic accretion.

1 Introduction

AM CVn stars are binary systems that have very short orbital periods that range from 5 to 65 minutes. These systems consist of white dwarfs accreting material from Roche lobe-filling companion star that usually is a lower-mass white dwarf star, but occasionally is a helium star. These systems are expected to be strong sources of gravitational waves (Nelemans et al., 2004). In this paper, we discuss the relationship between X-ray luminosity and orbital period for a sample of 28 AM CVn systems. We use the data from XMM, Chandra, and Swift observatories for collecting the X-ray flux and obtaining Orbital Period values from the literature. Studying the relationship between X-ray luminosity and orbital period can provide insights into the accretion process in AM CVn systems and techniques for searching for more of them.

2 Data and analysis

We collected the X-ray flux from Chandra, XMM-Newton, and Swift for all AM CVn systems listed in Table 1. Using the Chandra Source Catalog (CSC), we collected the flux from 0.5-7.0 keV from Release 2.0 (Evans et al., 2010) For XMM-Newton, using 4XMM-DR11, we collected the flux from 0.2-12.0 keV from Webb et al. (2020). For Swift, using the 2SXPS Swift X-ray telescope point source catalogue, we collected the flux from 0.3-10.0 keV from Tranin et al. (2022). We collected the distances from Gaia parallax measurements corrected for the Gaia zero-point offset, and which used Bayesian analysis to convert the measured parallaxes into inferred distances (Bailer-Jones et al., 2021). Using the flux we calculated the X-ray luminosity for each system. We also obtained the orbital periods of these systems from Ramsay et al. (2018). For the newly discovered AM CVn system, TIC 378898110, we collected the orbital period, X-ray flux and the distance from Green et al. (2023) In Table 1, we see that a few systems have periods estimated using superhumps. Superhump periods are typically within a few percent of the real periods, which is acceptable for the purposes of comparing luminosities with orbital periods. Using the uncertainty in the distances, we calculated 16% and 84% values for the luminosity. Using these values we made the error bars.

Our primary analysis involved plotting the X-ray luminosity versus the orbital period for the sample of AM CVn systems. Figure 1 shows a comparison between the observational data and a model prediction for X-ray luminosity from van Haaften et al. (2012),

$$L = \frac{GM_a}{2R_a} \frac{48}{5} \frac{G^{2/3}}{2c^5} \frac{M_a (9\pi)^2 10^{-6} M_\odot R_\odot^3}{\left(M_a + \frac{9\pi 10^{-3} \sqrt{\frac{M_\odot R_\odot^3}{2G}}}{P_{orb}} \right)^{1/3}} \frac{(2\pi)^{8/3}}{P_{orb}^{14/3}} \quad (1)$$

where M_a is the mass of the accretor, P_{orb} is the orbital period, and R_a is the radius of the accretor over the observed data. For plotting the predicted X-ray luminosity, we substituted the value of M_a as $0.8M_\odot$ from the work by Wong & Bildsten (2021) and that the luminosity generated in the boundary layer is 1/2 of the total accretion power, and all of the boundary layer luminosity goes into X-rays and the evolution of ultra-compact binaries by Nelemans et al. (2004); van Haaften et al. (2012)

We conduct a Spearman's rank correlation test for the sources that have the orbital period greater than 30 minutes, yielding a correlation coefficient of -0.48235 with a two-tailed p-value of 0.05846. This suggests a marginally significant association between the two variables. If we exclude the system SDSSJ0804+1616 and re-run the test, we obtained $r_s = -0.575$, with a two-tailed p-value of 0.02494, again marginally significant

Our findings also indicate that, at short orbital periods, the accretion rates are high enough to keep the system in a state at which the system is constantly accreting material from its companion star at a very high rate, where the bound-

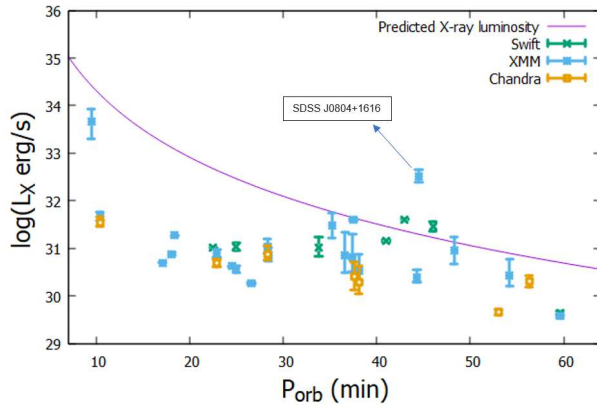


Figure 1: X-ray luminosity versus orbital period of selected AM CVn systems from Table 1.

ary layer is optically thick. In this regime, the X-rays produced at the white dwarf surface are thermalized into UV photons, leading to suppression of the X-ray emission, as seen in transient outbursts in dwarf novae (Wheatley et al., 2003).

Two systems stand out as overluminous relative to the trend of sources at similar orbital periods. One is V407 Vul, the shortest period object, which is a direct impact accretor (Marsh & Steeghs, 2002), which may lead to a higher fraction of its accretion power coming out in X-rays. The other is SDSS J0804+1616, which shows a strong magnetic field for the accretor, which may drive its orbital evolution to be faster than that due to gravitational radiation (Maccarone et al., 2023).

3 Conclusion

In conclusion, we observe that AM CVn systems with short orbital periods have X-ray luminosities below those from literature model predictions, but which, in hindsight, should have been anticipated given the expectation that bright systems will have optically thick boundary layers. We find a clear anti-correlation between X-ray luminosity and orbital period for the longer orbital period systems, in agreement with the theoretical expectations for the accretion process in these systems.

References

- Bailer-Jones, C. A. L., Rybizki, J., Fouesneau, M., Demleitner, M., & Andrae, R. 2021, *AJ*, 161, 147

- Evans, I. N., Primini, F. A., Glotfelty, K. J., et al. 2010, *ApJS*, 189, 37
- Green, M. J., Hermes, J. J., Barlow, B. N., et al. 2023, arXiv e-prints, arXiv:2311.01255.
- Maccarone, T. J., Kupfer, T., Najera Casarrubias, E., et al. 2023, arXiv e-prints, arXiv:2302.12318
- Marsh, T. R., & Steeghs, D. 2002, *MNRAS*, 331, L7
- Nelemans, G., Yungelson, L. R., & Portegies Zwart, S. F. 2004, *MNRAS*, 349, 181
- Ramsay, G., Green, M. J., Marsh, T. R., et al. 2018, *A&A*, 620, A141
- Tranin, H., Godet, O., Webb, N., & Primorac, D. 2022, *A&A*, 657, A138
- van Haaften, L. M., Nelemans, G., Voss, R., Wood, M. A., & Kuijpers, J. 2012, *A&A*, 537, A104
- Webb, N. A., Coriat, M., Traulsen, I., et al. 2020, *A&A*, 641, A136
- Wheatley, P. J., Mauche, C. W., & Mattei, J. A. 2003, *MNRAS*, 345, 49
- Wong, T. L. S., & Bildsten, L. 2021, *ApJ*, 923, 125

Star System	P_orb in mins	Log(X-Ray luminosity) in erg/sec	Chandra	Swift	Distance (in parsecs)	B_pc(84%)	b_pc(16%)
V407 Vul	9.5	33.66			4813.76	6584.68	3214.56
ESCet	10.4	31.67	31.55		1786.57	2013.34	1612.83
AM Cvn	17.1	30.7			300.02	303.06	297.24
SDSS J1908+3940	18.1	30.88			968.33	1004.87	935.96
HP lib	18.4	31.28			277.91	280.4	275.38
TIC 378898110	20.5			31.02	309.3	311.1	307.5
CX361	22.9	30.9	30.69		963.45	1058.7	878.92
CR Boo	24.5	30.63			349.55	353.67	344.79
KL Dra	25	30.56		31.04	907.92	985.06	829.11
V803 Cen	26.6	30.27			284.08	290.12	279.26
YZ LMi	28.3	31.04	30.89		815.72	994.31	694.03
CP Eri	28.4	30.86			725.62	874.06	623.87
V406 Hya	33.8			31.02	753.68	966.01	616.76
SDSS J1730+5545	35.2	31.49			1317.93	1771.03	977.98
V558 Vir	36.6(sh)	30.86			1548.05	2692.72	1015.78
SDSS J1240-0159	37.4	30.81			764.3	1358.88	544.51
NSV1440	37.5(sh)	31.6			1861.73	1917.21	1814.65
SDSS J1721+2733	38.1	30.54	30.29		674.02	997.94	510.86
ASASSN-14mv	41(sh)			31.15	247.06	253.23	240.59
ASASSN-14ei	43(sh)			31.61	256.89	259.87	253.71
SDSS J1525+3600	44.3	30.4			538.6	639.85	469.63
SDSS J0804+1616	44.5	32.51			998.97	1184.42	865.22
SDSS J1411+4812	46			31.46	452.01	502.2	397.95
SDSS J0902+3819	48.3	30.96			709	976.22	512.44
SDSS J1208+3550	53		29.66		210.7	223.64	198.89
SDSS J1642+1934	54.2	30.42			554.84	824.24	432.7
SDSS J1552+3201	56.3		30.31		422.52	481.38	369.72
SDSS J1137+4054	59.6	29.58		29.64	209.06	218.5	199.36

Table 1: Note: b_pc and B_pc refer to the lower and upper limit in the uncertainty in the the distances, respectively. Sh indicates that the orbital period was derived from superhumps.